Supporting Information

Thiam et al. 10.1073/pnas.1307685110

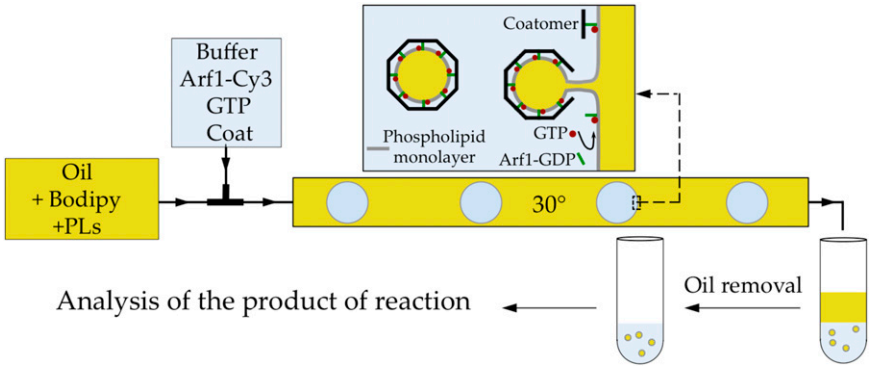

Fig. S1. Schematics of the buffer drop production and nanodroplet collection. The oil and buffer solutions, containing proteins, are used to fill two different syringes and injected using syringe pumps. Once in contact at the T connector, buffer drops are generated into the oil phase. Using this technique allows one to greatly increase the area of reaction in a controlled way. If the reaction with the coat protein complex I (COPI) machinery is positive, each drop will encapsulate the product of reaction, COPI decorated budded nanodroplets. At the extremity of the tube, the drops are collected; they separate from the continuous oil phase by buoyancy difference. The bottom fraction, which is the product of reaction, can be subsequently collected with a pipette and is ready for analysis.

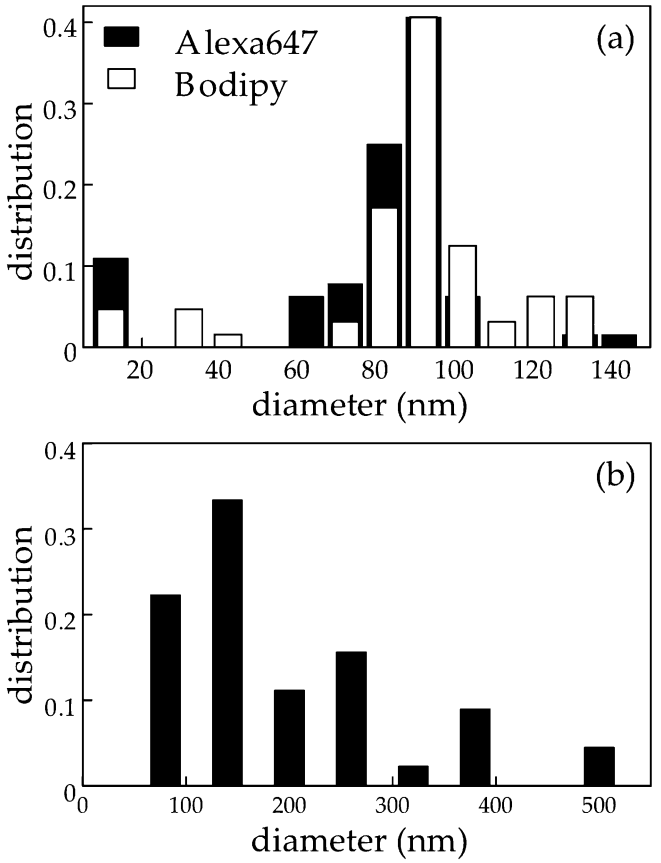

Fig. S2. Size distribution of the nanodroplets. (*A*) Size of nanodroplets determined by fluorescence cross-correlation spectroscopy (1). The distribution of cross-correlated oil and coatomer has a peak around 90 nm diameter for both the oil–Bodipy and coat–Alexa 647. This value is close to what is observed by EM. The inaccuracy arising from the fitting models adds a relative error in the diffusion times corresponding to 10–20 nm on the diameter, depending on the cross-correlation curve shape. (*B*) A sample of collected nanodroplets (with labeled oil and coatomer) is flattened on a glass coverslip. We then made movies of the motion of COPI–oil particles that we tracked in 2D and plotted the square displacement over time. The slopes of these curves, linear in most cases, equal twice the diffusion coefficient that is directly correlated to the size of the particle by the Stokes–Einstein law. Statistics for over 100 particles are presented here. The apparent distribution is likely to be shifted toward larger values because (*i*) we lose the 3D displacement and (*ii*) particles sometimes dock to the glass surface. The major size peaks around 100 nm in diameter. Similar results were also obtained by using different labels, either looking at colocalized signals of Arf–Cy3 and coatomer–Alexa 647 or Arf–Cy3 and oil–Bodipy.

1. Bacia K, Kim SA, Schwille P (2006) Fluorescence cross-correlation spectroscopy in living cells. *Nat Methods* 3(2):83–89.

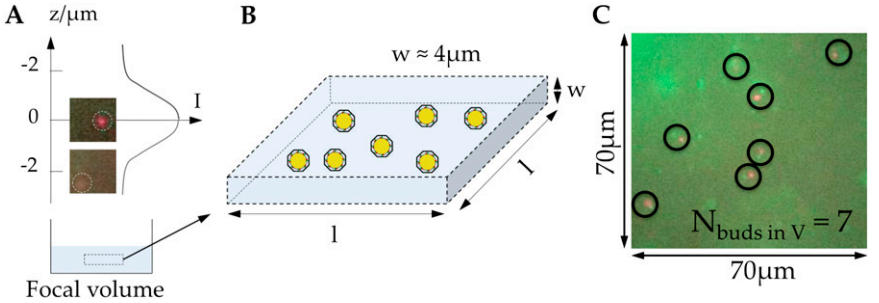

Fig. S3. Counting of the number of nanodroplets. The oil is labeled with 1% vol/vol Bodipy (excited at 488 nm). The coatomer is labeled with Alexa 647 (excited at 632 nm). The product of reaction is recovered as described in Fig. S2 and placed in a visualization chamber. The bottom of the chamber was made of glass coated with a thin layer of polymer (10 μm), polydimethylsiloxane; this minimizes the sticking of the particles. Focusing in the volume of the sample with a 63× objective mounted on a Zeiss confocal microscope [volume depth 4 μm (*A*), field of view of 140 ×140 μm (*B*)], we took snapshots every minute and counted the number of nanodroplets "moving" with the proteins. (*C*) Part of a snapshot with coat–oil spots moving together, circled spots (red, coat: green, oil). We count seven budded nanodroplets in this field. As shown in *A*, only coat spot intensities between 20–100% of the maximum signal were considered; they correspond to spots visible in the focal volume.

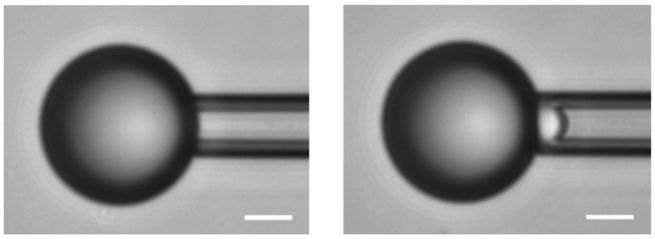

Fig. S4. Measurement of the surface tension with a micropipette. (*Left*) Droplet held with a glass micropipette as observed by optical microscopy. (*Right*) Droplet undergoing the maximum suction (hemispherical meniscus in the pipette) just before being fully aspirated in the pipette. (Scale bar, 10 μm.)

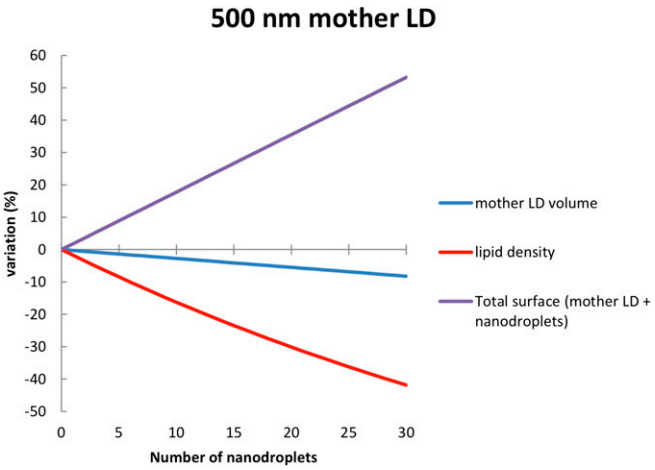

Fig. S5. Budding of nanodroplets consumes the phospholipid mixture (PL) monolayer. Each time a nano lipid droplet (LD) is formed and detached, the volume of the mother LD is slightly reduced (blue). Simultaneously, the total surface (mother LD + nano LDs, purple) increases dramatically. This leads to a fast decrease of the lipid packing on the mother lipid droplet with the number of budded nano LDs (red). In this chart, we assumed that nano LDs form and separate sequentially.

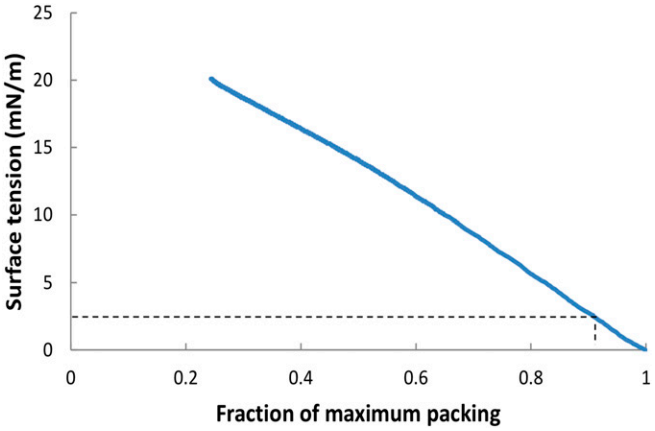

Fig. S6. Variation of the surface tension at the buffer/triacylglycerol (TAG) interface with the PL monolayer packing. The surface tension was measured with the packing as indicated in *Materials and Methods*. The dashed lines show that a very small variation in PL packing (less than 10% from maximum packing) is sufficient to increase the surface tension to 2 mN/m, which corresponds to the threshold above which the activity of COPI is reduced (Fig. 3*A*) and the hyperreactivity of the LD triggered (Fig. 3 *B* and *C* and Movies S2–S4). The error bars are 0.5 mN/m in surface tension and less than 2% in the packing variation.

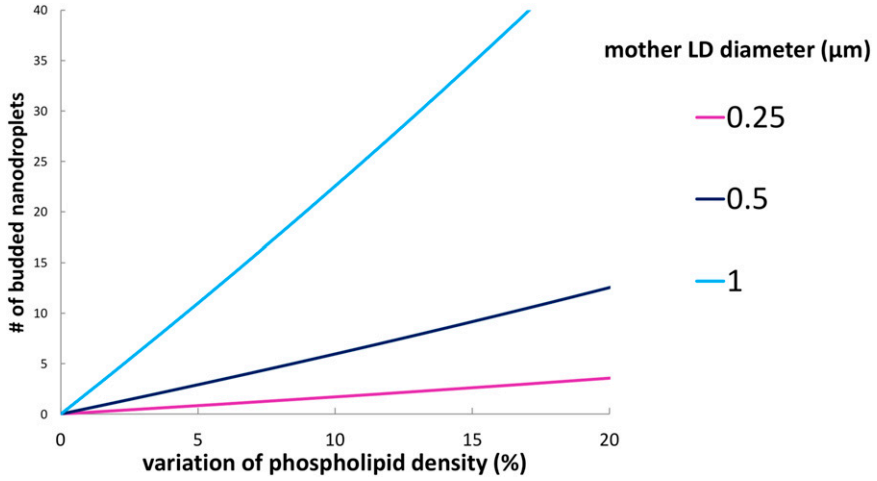

Fig. S7. Variation of PL packing with the number of budded nanodroplets. The graph shows the number of nano LDs that must be budded from the mother LD to reach a given variation of PL packing. This number increases with the size of the mother LD. For 10% variation of PL packing, only a few nano LDs have to be formed and detached from the mother LD. For instance, budding five nanodroplets reduces by 10% the packing of the phospholipids on a 500-nm mother droplet and makes it hyperreactive. The curves are convex because COPI depletes a quasi-constant percentage of PL. So, as events occur, the process becomes progressively less efficient.

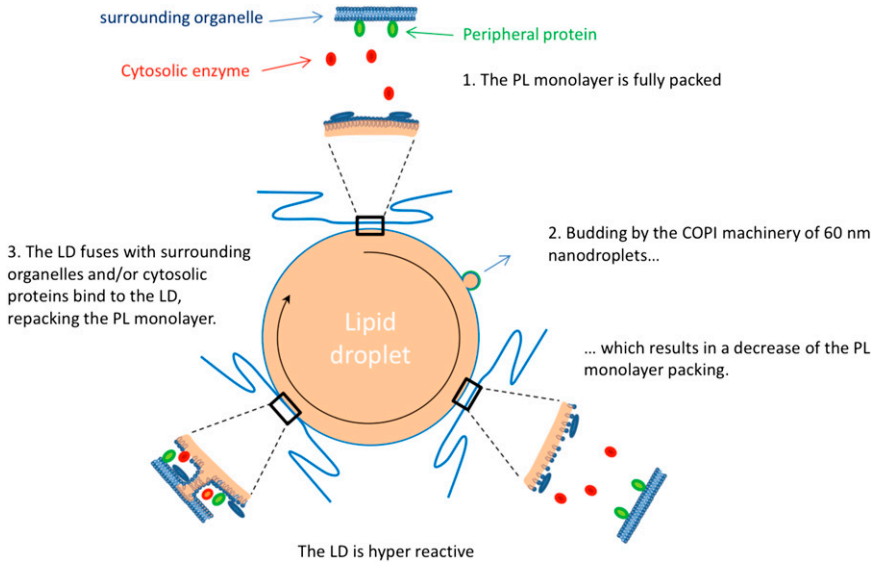

Fig. S8. Speculative model of the role of COPI on physiological lipid droplets. COPI-dependent relocation of proteins to/from LDs. Schematics of the COPI clamp model. (1) Initially, the PL monolayer of the LD (here a 500-nm LD) is fully packed. Some enzymes (in blue) are located on the LD. Others are cytosolic (red) or peripheral on other organelles (green). (2) Upon activation of the COPI machinery, nanodroplets are budded from the mother LD, inducing a decrease in PL packing and consequently an increase in surface tension. The mother LD becomes hyperreactive. (3) The LD fuses with the surrounding organelles and/or cytosolic enzymes directly bind to the LD interface and cover the unprotected TAG molecules. The PL monolayer is fully packed again with new enzymes at the LD surface.

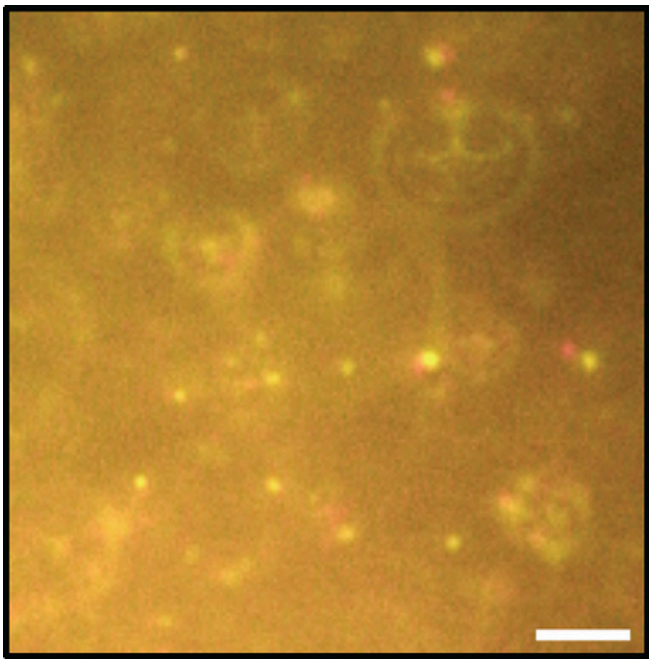

Movie S1. Spots showing Cy3–Arf1 (in green) and Alexa 647–coatomer (red) are cololocalized in the buffer drop. They move together (with a slight shift because of the time to switch the laser). The movie is in real time and the side of the picture is 140 μm.

Movie S1

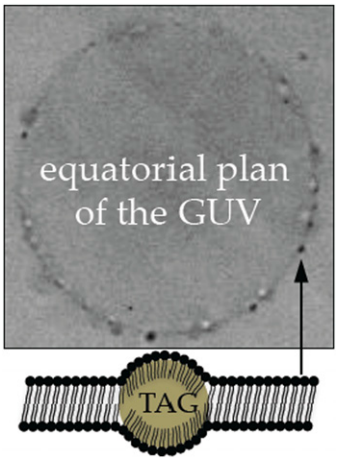

Movie S2. A 35-μm giant unilamellar vesicle (GUV) was incubated for 10 min with micrometer-scale LDs having a 0.3% PL/TAG ratio and observed under phase-contrast microscopy. The LDs have fused with the GUV and are trapped between the two leaflets, where they freely diffuse. The movie is in real time.

Movie S2

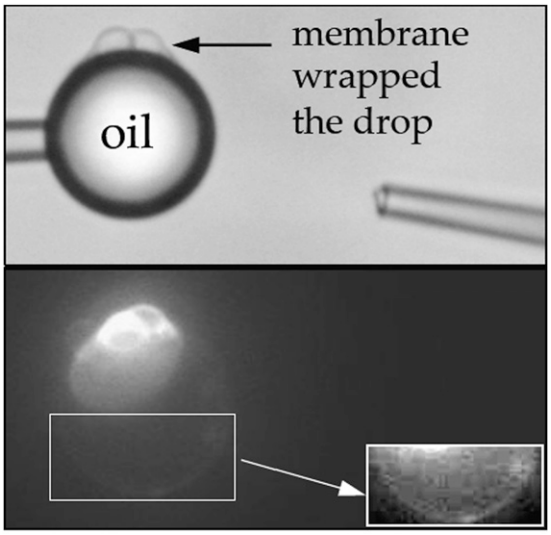

Movie S3. LDs (~30 μm) are micromanipulated in contact with a membrane mimicking small organelles. The PL/TAG ratio is 0.3%. The membrane immediately spreads on the LD.

Movie S3

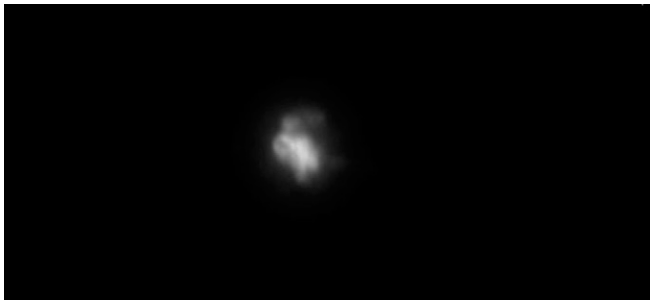

Movie S4. LDs (~30 μm) are micromanipulated in contact with a membrane mimicking small organelles. The PL/TAG ratio is 1%. The membrane ignores the LD and both the LD and the membrane remain intact.

Movie S4